

VĚDECKÉ SPISY VYSOKÉHO UČENÍ TECHNICKÉHO V BRNĚ

*Edice PhD Thesis, sv. 389*

*ISSN 1213-4198*

*thesis*  
**S**  
IS

*Ing. Jaroslav Jiruše*

**Investigations of Surface Structures  
of Materials by Low-Energy  
Electron Diffraction**

BRNO UNIVERSITY OF TECHNOLOGY

Faculty of Mechanical Engineering

Institute of Physical Engineering

**Ing. Jaroslav Jiruše**

**INVESTIGATIONS OF SURFACE STRUCTURES OF  
MATERIALS BY LOW-ENERGY ELECTRON DIFFRACTION**

URČOVÁNÍ STRUKTURY POVRCHŮ MATERIÁLŮ METODOU  
DIFRAKCE POMALÝCH ELEKTRONŮ

SHORT VERSION OF PH.D. THESIS

Study field: Physical and Material Engineering

Supervisor: Doc. RNDr. Petr Dub, CSc.  
Doc. RNDr. Tomáš Šikola, CSc.

Opponents: Prof. RNDr. Michal Lenc, Ph.D.  
RNDr. Karel Mašek, CSc.  
RNDr. Petr Jiříček, CSc.

Presentation date: 24. 6. 2004

**Key words**

LEED, low energy electron diffraction, surface structure, surfaces and thin films

**Klíčová slova**

LEED, difrakce pomalých elektronů, povrchová struktura, povrchy a tenké vrstvy

**Místo uložení**

Oddělení pro vědu a výzkum FSI VUT v Brně

© Jaroslav Jiruše, 2006

ISBN 80-214-3249-7

ISSN 1213-4198

## Table of Contents

1 GOALS OF THE THESIS .....	5
2 PRINCIPLE OF THE METHOD AND ITS PRESENT STATE .....	5
3 METHODS USED IN THE RESEARCH .....	7
4 MAIN RESULTS .....	9
4.1 Construction of an Apparatus .....	9
4.2 Tests of the Various Background Subtraction Methods .....	9
4.3 Limits of the Kinematic Analysis .....	11
4.4 Surface Structures Determined by Full Dynamical Analysis .....	13
4.4.1 <i>The Structure and Dynamics of the Al(110) Surface</i> .....	13
4.4.2 <i>Alkali Metal Adsorption on Al(110) Surface</i> .....	14
4.4.3 <i>Surface Reconstruction and Relaxation of Al(110)-c(2×2)-Na Structure</i> .....	15
4.4.4 <i>Determination of Al(110)-(4×1)-Na Structure</i> .....	18
4.4.5 <i>Structure of Al(110)-c(2×2)-Li and Formation of Surface Alloys</i> .....	21
5 SUMMARY .....	22
6 ZÁVĚR.....	24
7 AUTHOR'S PUBLICATIONS .....	25
8 REFERENCES .....	26
9 CURRICULUM VITAE .....	27



# 1 GOALS OF THE THESIS

Surface crystallography studies by Low-Energy Electron Diffraction (LEED) had been very rare in the Czech republic with practically no dynamical theory analysis before this work started. The principle aim of this research was to become acquainted both with up-to-date experimental and theoretical approaches of the LEED structure determination. The second aim was to investigate surface structures of clean metals and adsorbate systems.

# 2 PRINCIPLE OF THE METHOD AND ITS PRESENT STATE

Surface and interface physics has in recent decades become an important subdiscipline within the physics of condensed matter. It is the basic science for a number of advanced technologies, for instance the development of surface protective methods, semiconductor device technology, preparation of thin films and atomic clusters, nanotechnology etc. Within the surface science a special role is dedicated to the research of surface structures of materials. The resulted information is basic for many other research fields.

Low-Energy Electron Diffraction, a subject of this thesis, is a technique for investigation of well-ordered crystal surfaces [1, 2]. Electrons with the kinetic energy (hereafter just energy) typically up to 500 eV are directed towards a sample and are elastically scattered back with sufficient intensity only from surface atomic layers. This is caused by strong inelastic losses which limit the electron penetration depth. The de Broglie wavelength corresponding to this energy range varies from 0.6 to 1.7 Å which is of the order of interatomic distances in a solid. This makes LEED an almost ideal tool for the retrieval of surface structures assuming that the chemical composition of the sample is known.

The principle of the method is shown in Fig. 1. The electron beam generated by the gun hits the sample. By the interaction, the beam is scattered into particular directions, forming thus a diffraction pattern at the hemispherical fluorescent screen. From the symmetry of the diffraction pattern and the intensity of its individual spots, the structure of the sample is deduced.

The whole apparatus is placed inside the vacuum chamber because of electrons themselves as well as surface cleanness. Grids in front of the screen are charged in such a way that only elastically scattered electrons may approach the screen and that the space between the screen and the sample is free of electrostatic field.

The diffraction pattern consists of an array of spots. The pattern is a superposition of the reciprocal lattice projections corresponding to individual atomic layers of the sample. Since an eventual decomposition to the individual lattices of the real space is ambiguous, only basic information can be obtained from the shape of the diffraction pattern. To yield a complete 3D structure, one has to analyse intensities of diffraction spots as a function of accelerated voltage (or energy) of the incident electron beam (*intensity-voltage curves* or *intensity spectra*).

Calculations of structural parameters from the intensity spectra is not straightforward. A set of possible atomic coordinates and vibrational amplitudes is used as an input for the calculation of the theoretical intensity spectra which are compared with those measured experimentally. Depending on the quality of this fit, the assumed structural model is as a rule modified and a new calculation made. This trial and error procedure is repeated until a satisfactory agreement is obtained.

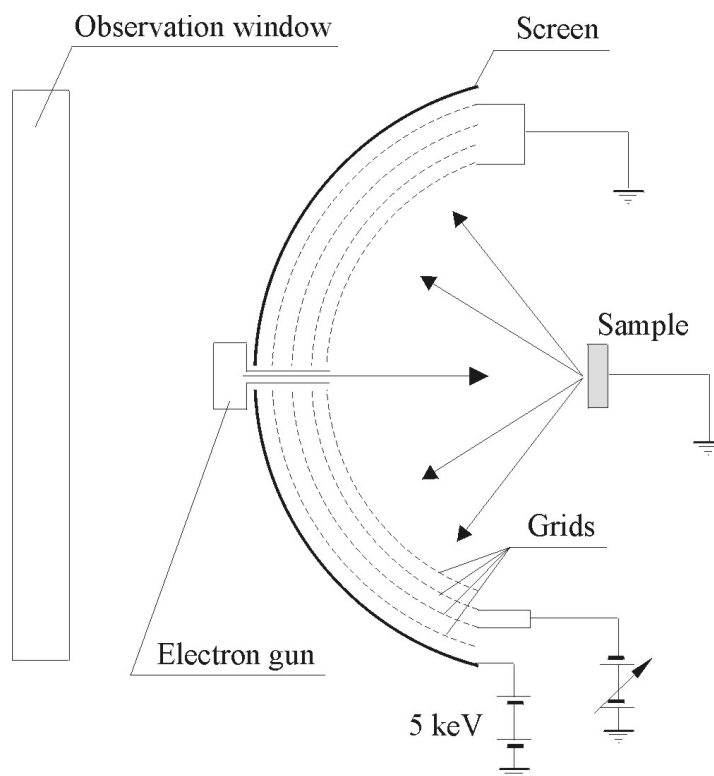


Fig. 1: Schematic of the LEED experimental apparatus.

The diffraction of electrons was experimentally discovered by C. J. Davisson and L. Germer [3] in 1927. Davisson was awarded the Nobel prize ten years later. The phenomenon began to be used for checking the crystallographic quality of prepared surfaces and for determinations of unknown surface structures three decades ago. The experimental setup has been continuously developing since then. Today's state of the art includes computer-controlled experiments performed in ultra-high vacuum conditions, fast data acquisition using a CCD camera, automated processing of pictures of the diffraction pattern to yield intensity spectra, computational analyses of intensity spectra with automated searches on powerful computers and joint measurements with other surface techniques on the same sample.

More than 1000 structures have been solved by LEED. It includes clean substrate surfaces, atomic and molecular adsorption on metals and semiconductors, coadsorption, disordered overlayers, adsorbate-induced relaxations and reconstructions, and even cluster-like bonding. Structures being solved now often involve complexities only dreamed 15 years ago.

### 3 METHODS USED IN THE RESEARCH

Experimental procedures were carried out as follows. Metal crystals used for analyses were cut from a single-crystal rod and aligned within  $0.1^\circ$  accuracy to the desired surface plane. Each sample had dimensions  $7 \times 5 \times 2$  mm. It was attached to the manipulator and installed in the vacuum chamber. The sample holder was connected via a copper braid to a liquid nitrogen reservoir providing cooling down the sample from room temperature to 100 K in about 30 minutes. The actual temperature of the sample was monitored by a thermocouple welded to its side. The sample could also be heated by a filament placed directly behind the sample. The vacuum chamber was pumped down to the pressure of the order  $10^{-9}$  Pa after standard procedures of heating and degassing.

The crystal surface was cleaned by means of sputtering by argon ions with an energy 0.5–2.0 keV. The ion current was 2–5  $\mu$ A. Actual sputtering times and ion energies depended on the crystal structure. The sputtering was followed by annealing to resume the ordering of the surface. The temperature of annealing depended on the sample.

Various alkali-metal adsorbates were deposited onto the crystal by evaporation from SAES sources [4]. Every source was mounted on a simple linear motion drive and approached during evaporation to the sample at a distance of several centimeters. The evaporation occurred by applying a current of several amps through the source. While the distance from the sample was fixed, the time and the current were varied to calibrate the source. We recognized the optimum coverage as a state when the ratio of integrated intensity of the fractional-order beams over the integral-order beams was highest (it is reasonable to suppose that well-ordered superstructure creates more intense diffraction spots than disordered ones). Typically, the exposure took 1–4 minutes with the current 5 A.

Pictures of the diffraction pattern were taken by a 16-bit Princeton CCD camera. The camera was cooled down to  $-40^\circ\text{C}$  to eliminate impuls noise. The camera sensitivity was calibrated by recording a digital image of the 99.5 % uniform light source.

The crystal was aligned with the electron gun and the screen to obtain normal incidence. This was done by rotating and tilting the crystal until the intensities of the symmetry equivalent beams became identical.

Measurements of series of diffraction images as a function of the electron acceleration voltage were controlled by a computer which commanded the LEED unit (setting acceleration voltage) as well as the camera (taking images) according to a prescribed energy range and step. Regressively, the computer took the information about the measured electron energy and current. Every taken image was saved on the disk including relevant information.

The cleanness of the crystal surface was always checked by Auger Electron Spectroscopy (AES) using AX100 electron spectrometer. The measurements were taken both before and after completion of a set of LEED measurements and it indicated that surface contamination by S, C and O elements was less than 0.03



monolayer. The presence of a superfluous magnetic field was also tested by observing the specular beam at off-normal incidence.

The saved pictures were further treated to obtain spot intensities. This image processing provided also compensation of errors both generated in the CCD camera and resulting from the imperfections of the fluorescent screen. It included radiometric corrections (i. e. the dark field and the flat field), a localization of diffraction spots (visually or calculated straightforwardly using knowledge of the substrate bulk structure), subtraction of the background, spot intensity evaluation and corrections to experimental conditions such as the magnitude of the electron beam current and the spot position on the hemispherical screen (Lambert's law). To make this task automatic a digital image acquisition and processing software was developed. The user-friendly interface design was written in Visual Basic and the computational routines were compiled as dynamically linked libraries using Visual Fortran. A special care was paid to the various methods of background subtraction (see Section 4.2).

After this data processing the resulting intensity spectra were prepared for an analysis. The quality of the measurement was judged by comparison of the intensity spectra of symmetry-equivalent beams, which should be identical. In practice, it turns out that the values of uncertainties of repetitive measurements are about 10 times smaller than the discrepancies between symmetry-equivalent beams. Therefore, it is almost useless to make repetitive measurements for the same condition of the sample surface and the same experimental setup.

Calculations of the theoretical intensity spectra proceed in three steps. First, the scattering of electrons by a single atom is calculated from the first principles of quantum mechanics. Then the atoms are arranged to form an atomic layer and scattering by the whole layer is computed. Finally, the layers are stacked into a crystal to yield the total diffraction. There are basically two theories to carry out the last two steps. Kinematic theory takes into account only single scattering events whereas dynamical theory includes multiple scattering of electrons within an atomic layer or between layers. The dynamical theory of LEED is in physical point of view more accurate but very complex and practically difficult to compute indeed. Therefore, we performed extensive tests of the use of the simpler kinematic approach (see Section 4.3). However, determinations of unknown structures (see Section 4.4) were carried out using full dynamical theory. Atomic scattering matrices were obtained using up to 18 phase shifts calculated from the muffin-tin band-structure potential of Moruzzi *et al.* [5]. They were renormalized for the effects of thermal vibrations using root-mean-square isotropic vibrational amplitudes of atoms. We estimate that the dynamical calculations were a numerically accurate reflection of the model assumptions to about 0.2 %, as determined by calculating the root-mean-square discrepancies between sets of intensity spectra calculated for different convergence criteria. All calculations used in the structure determination were carried out with full computer accuracy. We used codes of Pendry and his co-workers [1, 6] incorporated together with codes of Tong and Van Hove [7] and

further developed by Adams [8, 9] and we recompiled them for common personal computers (see the full version of the thesis for more detail).

The quality of the fit of calculated and measured intensity spectra was judged by a reliability factor ( $R$ -factor). Among various definitions, our  $R$ -factor was taken as a normalized sum of squares of discrepancies between the two spectra. It implies that  $R = 0$  for a complete agreement and  $R = 1$  for the sum of square discrepancies as big as the sum of measured square intensities itself. We use a single scaling constant between calculated and measured spectra for all beams simultaneously rather than a set of beam-dependent scaling constants. Thus a good agreement in our analyses includes not only the correct shapes of individual spectra but also the relative intensities between the beams, even in the case where they differ by a factor of 200 (an example of plots is given in Section 4.4.3).

## **4 MAIN RESULTS**

### **4.1 CONSTRUCTION OF AN APPARATUS**

In the first stage of this work the author learned some experiences of LEED technique from his 6 months study stay at Aarhus University in Denmark. However, the corresponding experimental equipment was missing in Brno, therefore, the author was involved in its development, naturally.

First, an analytical apparatus consisting of LEED and an elipsometer was built. The design met the objectives to carry out ellipsometry analyses without interrupting the vacuum in the analytical chamber while exchanging a sample. This was ensured by a prepumped chamber together with a storage chamber with a carousel of a capacity 6 samples. The LEED unit in the apparatus was donated by Technical University of Eindhoven and was used for checking the crystallographic quality of prepared surfaces only. This unit could not be used for the measurements of LEED intensity spectra.

A complete LEED experiments were carried out in laboratories at the Aarhus University. Later on a commercial Omicron LEED facility was built by my colleagues into the ultra-high vacuum system at the Institute of Physical Engineering in Brno. At the present time the complete LEED experiment can be run at this institute and the approaches discussed in this thesis utilized.

### **4.2 TESTS OF THE VARIOUS BACKGROUND SUBTRACTION METHODS**

As mentioned in Section 3, the background subtraction is one of the substantial steps in processing of diffraction patterns. An impact of various methods on the determination of structural parameters was analyzed on the example of Al(111) surface structure. The tested methods include:

*Approximation by average value on the border* [10] assumes the background intensities constant within the spot area. The value of the background is defined as the arithmetic average of pixel values along the border of the delimiting square. This value is then subtracted from each pixel value within the spot area.

*Approximation by average value on the border of the quadrants* [11] assumes the constant background in each quadrant of the delimiting square. We calculate the arithmetic average of the pixel values along the outer border of every quadrant. This value is then subtracted from the pixel values within the corresponding quadrant.

*Approximation in rows and columns.* Here, it is supposed a background whose intensity changes linearly either in rows or columns. The intensity values of pixels lying in a row (column) connecting two opposite border pixels are then given by linear interpolation between values of those two pixels [12].

*Approximation by a 3D surface.* This method interpolates the background values by two-dimensional quadratic forms with boundary conditions given by the border pixel values. Two different forms were used:

$$B(i, j) = a_0 + a_1 i + a_2 j + a_3 ij \quad (4 \text{ coefficients}),$$

$$B(i, j) = a_0 + a_1 i + a_2 j + a_3 ij + a_4 i^2 + a_5 j^2 \quad (6 \text{ coefficients}),$$

where  $B$  is the background value and  $i$  and  $j$  are pixel coordinates. The coefficients  $a_0, \dots, a_5$  in these formulas are evaluated by the least-squares method.

*Expansion of minimum.* The pixel values on the border of the delimiting square are considered as the background values. Hence, one can let them expand into the area of the diffraction spot. This is done by the convolution filtering of image pixel values. A square of  $3 \times 3$  pixels is taken as a filter. Within this square around a processed pixel, the minimum pixel value is found and taken as the background value in the processed pixel. This must be done several times to let the values expand from the border to the centre of the spot area. The number of repetitions depends on the width of the square delimiting the diffraction spot [13].

The series of diffraction images of Al(111) surface was taken in the electron energy range 50–350 eV with the step 1 eV. The resulting images were treated by various background subtraction methods to yield diffraction spot intensities. The intensities of symmetry-equivalent spots were averaged to obtain five final intensity spectra, namely for (01), (0 -1), (-21), (02) and (0 -2) non-equivalent spots. The standard full-dynamical calculations were applied to these intensity spectra to test the impact of the background subtraction on the LEED structural analysis.

The resulting structural parameters are compared in Tab. 1. One can see here that, the first four background subtraction methods in the table lead to the equivalent results. Contrary to that, the method of expansion of minimum gave unacceptable values of the vibrational amplitudes and the higher  $R$ -factor. Also its intensity spectra were considerably higher by nearly constant amount than the others. The approximation by a 3D surface with 6 coefficients gave us values only slightly different and within the accuracy limits.

We also prepared a testing series of artificial images (that is, of known intensities) biased by Gaussian distributed noise. The corresponding conclusion (see the full

version of the thesis) was in agreement with that obtained from Tab. 1: four methods gave approximately the same results, a little too complicated approximation by a 3D surface with 6 coefficients differed within accuracy limits and expansion of minimum did not give reasonable results.

Hence, the last two methods are not recommended for application in LEED. It is recommended to choose as simple a method as possible, i. e. the linear approximation in rows or in columns. We used this method in all subsequent analyses.

	Border	Quadrant	Rows/col.	4-coeff.	6-coeff.	Minimum
$d_{12}$ [Å]	2.36	2.36	2.36	2.36	2.36	2.34
$d_{23}$ [Å]	2.32	2.32	2.32	2.32	2.33	2.28
$d_{34}$ [Å]	2.35	2.35	2.35	2.35	2.34	2.39
$u_1$ [Å]	0.16	0.16	0.16	0.16	0.17	0.02
$u_{bulk}$ [Å]	0.08	0.08	0.08	0.08	0.09	0.002
$V_{im}$ [eV]	5.3	5.2	5.2	5.1	4.9	5.7
$R$	0.024	0.023	0.023	0.022	0.036	0.059

Tab. 1: Comparison of the structural parameters of Al(111) surface structure calculated from intensity spectra obtained for 6 different background subtraction methods.  $d_{12}$ ,  $d_{23}$  and  $d_{34}$  denote interlayer spacings among the first four layers (from surface to bulk),  $u_1$  and  $u_{bulk}$  are root-mean-square vibrational amplitudes of atoms in the first layer and the bulk, respectively,  $V_{im}$  is the electron damping energy and  $R$  denotes the total  $R$ -factor (normalized sum of squares).

### 4.3 LIMITS OF THE KINEMATIC ANALYSIS

As mentioned in Section 3, there is a big gap in complexity between kinematic and dynamical theories. Therefore, we tried to apply the kinematic approach for the determination of structural parameters of Ni(100), Ni(100)-c(2×2)-Na and Al(111) surfaces. The results were compared with those obtained by the full dynamical theory [14, 15]. We supposed that in cases when we need only a rough estimation of surface structural parameters, it would be reasonable to treat experimental data by this easier method. The kinematic formula were slightly adapted to use electron damping energy as an imaginary part of the complex inner potential (see the full version of the thesis). Structural search was automated using Marquardt optimization procedure [16]. All computations were written in Fortran programming language.

Resulted parameters of three surface structures are listed in Tab. 2 for both kinematic and dynamical approaches. Investigation of the Ni(100) structure revealed that both theories are in agreement in a prediction of interlayer spacings. Kinematic vibrational amplitudes are greater than dynamical ones. It is a general feature of

LEED that the method is more sensitive to the determination of the structure than to the finding the vibrational amplitudes.

Ni(100)-c(2×2)-Na structure was a hard test of our method. Some authors say that the agreement of the structure calculations with the LEED experiment is much worse in the case of adsorbed alkali atoms than for clean metals. Therefore, it is suggested in [17] that the theoretical model can be improved by inclusion of the electric dipole between substrate and superstructure which breaks the spherically symmetrical potential. Surprisingly, the results in Tab. 2 show a good agreement between the two theories, even for vibrational amplitudes.

Contrary to the previous case, our computational model gave a systematic error in the determination of interlayer spacings for Al(111) structure, mainly too big contraction between the first and the second layer. Taking into account that the dynamical calculations were performed on the same experimental data, the non negligible systematic errors generated by the kinematic model are present.

	Ni(100)		Ni(100)-c(2×2)-Na		Al(111)	
	Kinematic	Dynamical	Kinematic	Dynamical	Kinematic	Dynamical
$d_{12}$ [Å]	1.79	1.77±0.01	2.42	2.38±0.04	2.07	2.36±0.01
$d_{23}$ [Å]	1.74	1.76±0.01	1.74	1.74±0.01	2.33	2.33±0.01
$u_1$ [Å]	0.22	0.16±0.02	0.22	0.25±0.02	0.29	0.13±0.02
$u_2$ [Å]	0.12	0.10±0.01	0.14	0.13±0.02	0.12	0.08±0.01
$u_{bulk}$ [Å]	0.08	0.10±0.01	0.09	0.09±0.01	0.07	0.08±0.01
$R$	0.107	0.015	0.108	0.045	0.085	0.009

Tab. 2: Comparison of kinematic and dynamical results for Al(111), Ni(100) and Ni(100)-c(2×2)-Na structures. The denotation of parameters is the same as in Tab. 1. The bulk interlayer spacing is 1.762 Å and 2.331 Å for nickle and aluminium substrates, respectively. Dynamical data are taken from [14, 15].

Thus the success of the kinematic approach did not depend on the complexity of the structures. Our most complex structure gave the best results. Despite the errors, the rough treatment of experimental data by the described method gave us the useful estimation of the structural parameters of the solid surfaces. The computer code based on the kinematic scattering theory was simpler and easier to use than that built on the dynamical description of scattering processes. Therefore, it was recommended to use kinematic results as input data into the dynamical structural search to speed up computational times.

However, the above successes have been counterbalanced by some limitations. The basic failure of the kinematic theory lies in the restriction to the integral-order beams only. In the systems with superlattices there appear the fractional-order beams, being absent for the (1×1) surface. Since in the kinematic limit the (1×1) substrate cannot contribute to the extra beams, no interlayer interference is present.

It follows that the intensity should be a decreasing function of energy. However, the experiment shows that the intensity spectra of the fractional-order beams contain many peaks similar to the spectra of the integral-order beams. It is clear that for the calculation of the fractional-order beam intensity, the kinematic theory cannot be used. Thus the dynamical approach is irreplaceable.

## 4.4 SURFACE STRUCTURES DETERMINED BY FULL DYNAMICAL ANALYSIS

### 4.4.1 The Structure and Dynamics of the Al(110) Surface

The Al(110) surface has played an important role in the development of experimental and theoretical methods for the study of surface relaxations. A large contraction –10 % of the first interlayer spacing was first reported in the pioneering LEED study of Jepsen *et al.* [18] in 1972. A long discussion has been passing since then about properties of multilayer relaxation. Recently, Marzari *et al.* [19] have presented *ab initio* calculations of the temperature dependence of surface relaxations and vibrational amplitudes of the Al(110) surface using ensemble density-functional molecular dynamics. Their results conclude that the first and second interlayer spacings exhibit negative and positive coefficients of thermal expansion, respectively, and that the surface-normal vibrations of second layer atoms are larger than those of first layer atoms. Thus we performed a new LEED study of this system using measurements at 100 K and 300 K in order to provide the experimental basis for an evaluation of new theories.

The measurements were carried out in a commercial  $\mu$ -metal ultra-high vacuum chamber with a base pressure less than  $10^{-8}$  Pa. The initial cleaning of the aluminium sample was carried out by sputtering by argon ions with energy 2.5 keV for 3 hours. After that the daily maintenance of the sample consisted of 1 hour sputtering by  $\text{Ar}^+$  with energy 500 eV (the ion current was 2.5  $\mu\text{A}$  and the pressure in the chamber was less than  $3 \times 10^{-4}$  Pa) followed by 20 minutes annealing at 670 K (the pressure was less than  $1 \times 10^{-7}$  Pa). It should be particularly noted that the annealing temperature used for the Al(110) face was 50 K lower than that commonly used for the more close-packed Al faces (111) or (100). The open (110) surface tends to restructure at higher temperatures, which results in faceting.

Intensity spectra were measured at 100 K and 300 K for the clean Al(110) surface at normal beam incidence in the electron energy range of 50–450 eV with a step size of 1 eV. Spectra were recorded for 33 beams, consisting of all excited beams having an energy range greater than about 30 eV, except for a few beams whose spots on the fluorescent screen were overlapped by the shadow of the connections to the electron gun.

Intensities of the diffracted beams were calculated by the full dynamical theory of electron diffraction (see the full version of the thesis for details). The  $L$ -space and  $k$ -space treatments, respectively, of multiple scattering within and between the atomic

layers parallel to the surface involved the use of up to 324 partial waves and 161 beams (reduced due to the symmetry of normal incidence to 48 beams). The lattice constants for aluminium were taken to be 4.0341 Å for 100 K and 4.0496 Å for 300 K [20].

Resulting structural parameters are listed in Tab. 3. It confirms the theory prediction [19] that the contraction of the first interlayer spacing and the expansion of the second interlayer spacing increase with temperature. Further it acknowledges that the vibrational amplitudes of aluminium atoms in the first two layers are significantly larger than for atoms in deeper layers. Finally, it validates a surprising fact that atoms in the second layer have larger vibrational amplitudes than atoms in the first layer at 300 K. This may be explained by presence of an “easy channel” for vibrations on the open Al(110) surface in the surface-normal direction.

Clean Al(110)		
	T = 100 K	T = 300 K
$d_{12}$ [Å]	1.31±0.03	1.27±0.03
$d_{23}$ [Å]	1.51±0.03	1.53±0.03
$d_{34}$ [Å]	1.37±0.02	1.37±0.03
$d_{45}$ [Å]	1.44±0.02	1.43±0.03
$u_1$ [Å]	0.17±0.04	0.25±0.03
$u_2$ [Å]	0.17±0.08	0.29±0.06
$u_3$ [Å]	0.12±0.04	0.18±0.03
$u_{bulk}$ [Å]	0.07±0.02	0.14±0.01
$R$	0.0376	0.0402

Tab. 3: Final parameter values of Al(110) structure at 100 K and 300 K. The interlayer spacings and atomic vibrational amplitudes are denoted  $d_{ij}$  and  $u_i$ , respectively, where the subscripts indicate the layers in question. The quality of the fit is given by the reliability factor  $R$  defined in Section 3.

#### 4.4.2 Alkali Metal Adsorption on Al(110) Surface

Behavior of alkali metals on metal surfaces is an important testing ground for theories of adsorption [21]. The interplay between experiment and *ab initio* theories of adsorption is crucial for further development of this branch of science. The adsorption of alkali metals on Al(110) surface is of particular interest because the extrapolation of the results of previous studies of adsorption has led to quite different expectations. Thus, on the one hand, alkali metal adsorption on Al(111) and Al(100) at room temperature leads to a substitutional reconstruction of the substrate. On the other hand, small coverages of alkali metals on (110) surfaces of Ni, Cu, Ag and Pd induce (1×2), “missing-row” reconstructions.

Our measurements indicate that Al(110) does not follow the pattern of other fcc(110) metals in forming  $(1 \times 2)$  missing-row structures. However, the adsorption behaviour also differs in many respects from that found for Al(111) and Al(100). We have extensively studied the adsorption of Na and Li on Al(110). Adsorbed Na leads with increasing coverage gradually to the formation of  $(3 \times 2)$ ,  $c(2 \times 2)$ ,  $(3 \times 1)$ ,  $(4 \times 1)$  and  $(2 \times 1)$  phases. Only the  $c(2 \times 2)$  and  $(4 \times 1)$  phases are well ordered. Adsorption of Li leads to a similar sequence of phases as sodium except that for Li there is no  $(4 \times 1)$  phase. Thus the only well-ordered structure is  $c(2 \times 2)$  phase. All three well-ordered phases of Na and Li were analyzed and for the first time quantitatively determined as described in the next three sections.

#### 4.4.3 Surface Reconstruction and Relaxation of Al(110)- $c(2 \times 2)$ -Na Structure

The measurements were carried out in the same way as in the case of clean Al(110) surface. A sharp  $c(2 \times 2)$  LEED pattern with a good contrast is obtained after the deposition of 0.5 monolayer of Na. An optimally developed  $c(2 \times 2)$  structure can also be obtained by adsorption of more than 0.8 monolayer followed by annealing to 410 K. Desorption of Na occurs at temperatures higher than 475 K with restoration of the original  $(1 \times 1)$  LEED pattern. The annealing procedure was used to prepare the  $c(2 \times 2)$  phase for which quantitative LEED measurements were performed in this study.

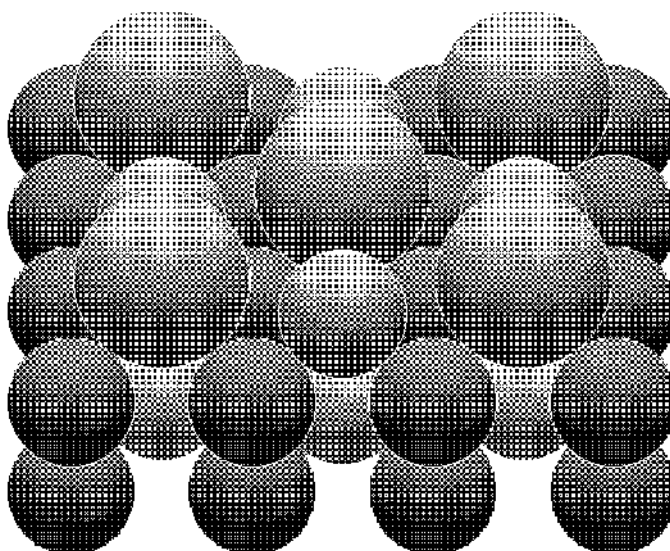


Fig. 2: A model of the Al(110)- $c(2 \times 2)$ -Na structure (side view tilted by  $45^\circ$  from the plane of the paper).



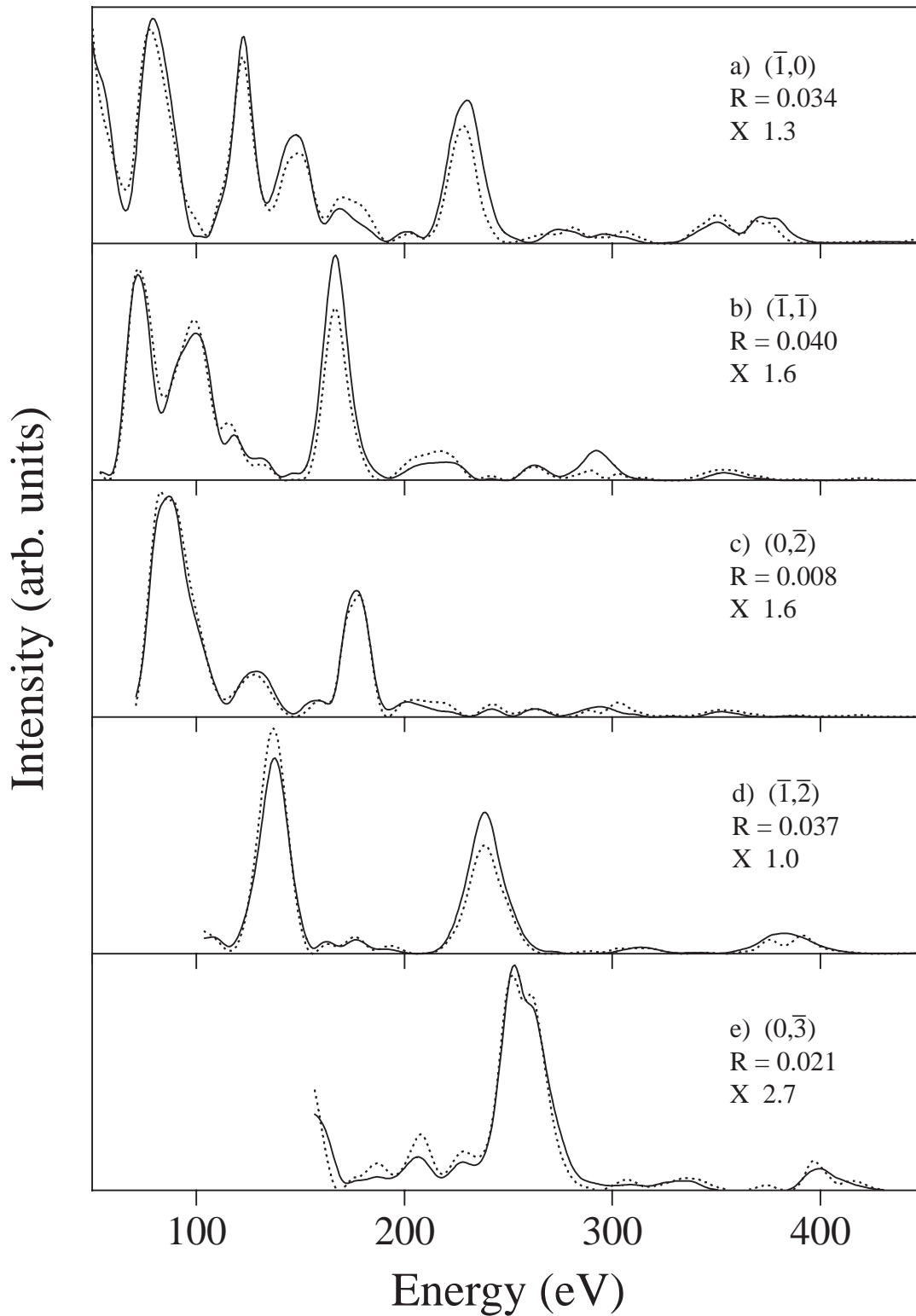


Fig. 3: Comparison of experimental (solid lines) and calculated (dotted lines) intensity spectra for Al(110)-c(2×2)-Na structure for 5 diffracted beams at normal incidence of the primary beam. The beam (hl) indices,  $R$ -factors, and scale factors are shown in each panel.

Intensity spectra were measured at 100 K, in the energy range 40–440 eV with a step size of 1 eV, both at normal incidence and at off-normal incidence  $\theta = 10^\circ$ . Intensity spectra were recorded for a total of 25 symmetry-inequivalent beams at  $\theta = 0^\circ$  (15 integral-order and 10 fractional-order) and 32 symmetry-inequivalent beams at  $\theta = 10^\circ$  (18 integral-order and 14 fractional-order).

LEED intensities were again calculated using the full dynamical theory of LEED. At the highest energy 324 partial waves and 321 plane waves (reduced by symmetry to 88 and 171 symmetry-adapted plane waves at  $\theta = 0^\circ$  and  $\theta = 10^\circ$ , respectively) were used in the  $L$ -space and  $k$ -space treatments, respectively, of multiple scattering within and between the atomic layers parallel to the surface.

Al(110)–c(2×2)–Na			
	$\theta = 0^\circ$	$\theta = 10^\circ$	Average
$d_{01}$ [Å]	1.06±0.03	1.05±0.03	1.06±0.02
$d_{12}$ [Å]	1.28±0.02	1.25±0.02	1.27±0.01
$d_{23}$ [Å]	1.35±0.03	1.37±0.03	1.36±0.02
$d_{34}$ [Å]	1.36±0.03	1.35±0.03	1.36±0.02
$d_{45}$ [Å]	1.38±0.03	1.38±0.03	1.38±0.02
$d_{56}$ [Å]	1.40±0.03	1.40±0.05	1.40±0.03
$d_{67}$ [Å]	1.42±0.04	1.41±0.06	1.42±0.03
$\Delta r_3$ [Å]	0.15±0.03	0.14±0.02	0.14±0.02
$\Delta r_5$ [Å]	0.06±0.04	0.05±0.05	0.06±0.03
$u_0$ [Å]	0.27±0.04	0.27±0.03	0.27±0.02
$u_1$ [Å]	0.17±0.04	0.17±0.03	0.17±0.02
$u_2$ [Å]	0.13±0.04	0.13±0.03	0.13±0.02
$u_{3A}$ [Å]	0.17±0.04	0.14±0.04	0.16±0.03
$u_{3B}$ [Å]	0.11±0.04	0.09±0.04	0.10±0.03
$u_4$ [Å]	0.10±0.04	0.10±0.04	0.10±0.03
$u_5$ [Å]	0.11±0.04	0.10±0.04	0.10±0.03
$u_{bulk}$ [Å]	0.10±0.04	0.15±0.10	0.11±0.04
$R$	0.039	0.045	

Tab. 4: Final parameter values for the Al(110)–c(2×2)–Na structure. The interlayer spacings and vibrational amplitudes are denoted  $d_{ij}$  and  $u_i$ , respectively, where the subscripts indicate the layers in question (0 belongs to the overlayer and 1 to the first layer of the substrate). The third and the fifth Al layers are split into bilayers with vertical splittings denoted by  $\Delta r_3$  and  $\Delta r_5$ .

In the process of the structure determination, only the model with Na atoms adsorbed in two-fold substitutional site was able to reproduce the experimental data while models with on-top, two-fold hollow, two-fold short and long-bridge sites and

two-fold substitutional site with readsorption of displaced Al atoms in high symmetry sites were all wrong. Hence, it was assumed that the displaced Al atoms are readsorbed at surface steps. The  $R$ -factors for the discarded models were in the range of 0.25–0.35 as compared to the value of 0.045 found for the optimal model.

A hard sphere model of the Al(110)–c(2×2)–Na structure is shown in Fig. 2. Plots of some of the intensity spectra are shown in Fig. 3. The results of independent refinements for measurements at  $\theta = 0^\circ$  and  $\theta = 10^\circ$  are listed in Tab. 4. As can be seen, a good agreement exists between the two sets of results. Na is found to adsorb in two-fold substitutional sites with a displacement of one-half monolayer of Al atoms from the top layer of the substrate. The Na-Al interlayer spacing is 1.06 Å, corresponding to a hard-sphere radius of 1.62 Å for the adsorbed Na atoms, as compared to the bulk bcc radius of 1.86 Å. The reconstructive adsorption leads to strong perturbations of the substrate structure extending to the fifth Al layer. A large rumpling 0.14 Å of the third Al layer is found, together with a smaller rumpling 0.06 Å of the fifth layer. Atoms in the third Al layer which are directly below Na atoms exhibit enhanced vibrations as compared to the remaining atoms of the layer.

#### 4.4.4 Determination of Al(110)–(4×1)–Na Structure

The structure was prepared using the same source as for c(2×2)–Na structure and experimental conditions hold as well. Sharp (4×1) LEED patterns with good contrast were obtained after deposition of 0.8 monolayer of Na at room temperature and subsequent brief annealing to 380 K to partially desorb Na. Optimal development of the (4×1) phase was achieved by carrying out measurements of intensity spectra after successively annealing for 2 min at increasing temperatures in the range 370–390 K until the ratio of integrated intensity in intensity spectra for fractional-order and integral-order beams reached a maximum. The structure could also be formed by adsorption of 0.75 monolayer of Na at room temperature. However, since the structure occurs in a narrow coverage range, it proved to be easier to prepare it by annealing.

The intensity spectra used for the analysis were measured at 100 K and at normal incidence in the energy range 40–340 eV with a step size of 1 eV. The spectra were taken for a total of 35 symmetry-inequivalent beams. In the intensity calculations, at the highest energy, 324 partial waves and 415 plane waves (reduced by symmetry to 117 symmetry-adapted plane waves), were used in the  $L$ -space and  $k$ -space treatments, respectively, of multiple scattering within and between the atomic layers parallel to the surface.

A full optimization of the fit between experimental and calculated intensities revealed that the structure contains 1/4 monolayer of Na atoms adsorbed in substitutional sites formed by displacing 1/4 monolayer of Al atoms from the first layer of the substrate, together with 1/2 monolayer of Na atoms adsorbed in four-fold hollow sites on the first Al layer.

Al(110)-c(4×1)-Na						
Layer	Atom	$x$ [Å]	$y$ [Å]	$z$ [Å]	$d_{ij}$ [Å]	$u$ [Å]
1	Na	3.95±0.08	$a_0/2$	2.09±0.03	1.27±0.03	0.30±0.03
	Na	-3.95±0.08	$a_0/2$	2.09±0.03		0.30±0.03
	Na	0	0	1.01±0.03		0.28±0.05
	Al	$\sqrt{2} a_0$	0	0.10±0.03		0.18±0.03
	Al	2.86±0.09	0	0		0.16±0.04
	Al	-2.86±0.09	0	0		0.16±0.04
2	Al	1.41±0.09	$a_0/2$	-1.27±0.03	1.40±0.03	0.15±0.05
	Al	-1.41±0.09	$a_0/2$	-1.27±0.03		0.15±0.05
	Al	4.29±0.09	$a_0/2$	-1.30±0.03		0.16±0.04
	Al	-4.29±0.09	$a_0/2$	-1.30±0.03		0.16±0.04
3	Al	0	0	-2.69±0.03	1.38±0.03	0.13±0.06
	Al	2.81±0.10	0	-2.75±0.03		0.11±0.05
	Al	-2.81±0.10	0	-2.75±0.03		0.11±0.05
	Al	$\sqrt{2} a_0$	0	-2.76±0.03		0.11±0.05
Bulk	Al					0.12±0.06

Tab. 5: Atomic coordinates ( $xyz$ ) and rms vibrational amplitudes  $u$  determined for the Al(110)-(4×1)-Na structure. The  $x$  and  $y$  axes lie in the surface plane along the [-110] and [001] directions, respectively. The  $z$ -axis is the outward surface normal. Interlayer spacings  $d_{ij}$  are also given. For comparison, the bulk interlayer spacing is  $\sqrt{2} a_0 / 4 = 1.4263$  Å, and that bulk Al positions in the  $x$  direction are at 0 Å,  $\sqrt{2} a_0$  and  $\pm \sqrt{2} a_0 / 2 = \pm 2.8525$  Å in odd-numbered layers, and at  $\pm \sqrt{2} a_0 / 4 = 1.4263$  Å and  $\pm 3\sqrt{2} a_0 / 4 = \pm 4.2788$  Å in even-numbered layers, where the bulk lattice constant at 100 K is  $a_0 = 4.0341$  Å. The reliability factor is  $R = 0.063$ .

Resulting parameters are listed in Tab. 5. A hard-sphere model of the substitutional (4×1)-Na structure based on the structural parameters from Tab. 5 is shown in Fig. 4. As can be seen, the final refinement of the structure led to displacements of 0.33 Å parallel to the surface in the [-110] direction, of two of the three Na atoms in the unit cell from the four-fold hollow sites to positions of lower symmetry. This is a consequence of the size of the Na atoms, which are too large to simultaneously occupy the two high-symmetry sites separated by only 2.85 Å. These two Na atoms have an effective hard-sphere radius of 1.68 Å, whereas the substitutionally adsorbed Na atom has a hard-sphere radius of 1.60 Å. Vertical relaxations of substrate atoms, and lateral relaxations in the [-110] ( $x$ ) direction, were considered for the first five Al layers, consistent with the p2mm symmetry of

the  $(4\times 1)$ -Na phase. For the substrate layers, the  $(4\times 1)$  unit cell contains four Al atoms in three inequivalent positions. As can be seen from the results in the Tab. 5, lateral relaxations were less than the estimated uncertainties in the atomic coordinates. However, significant vertical displacements were found between the  $(4\times 1)$ -Al sublattices in the first three Al layers. It can be noted in particular that the Al atoms lying directly beneath substitutionally adsorbed Na atoms are displaced towards the surface by  $0.06\text{--}0.07\text{ \AA}$  with respect to the other Al atoms in the third layer.

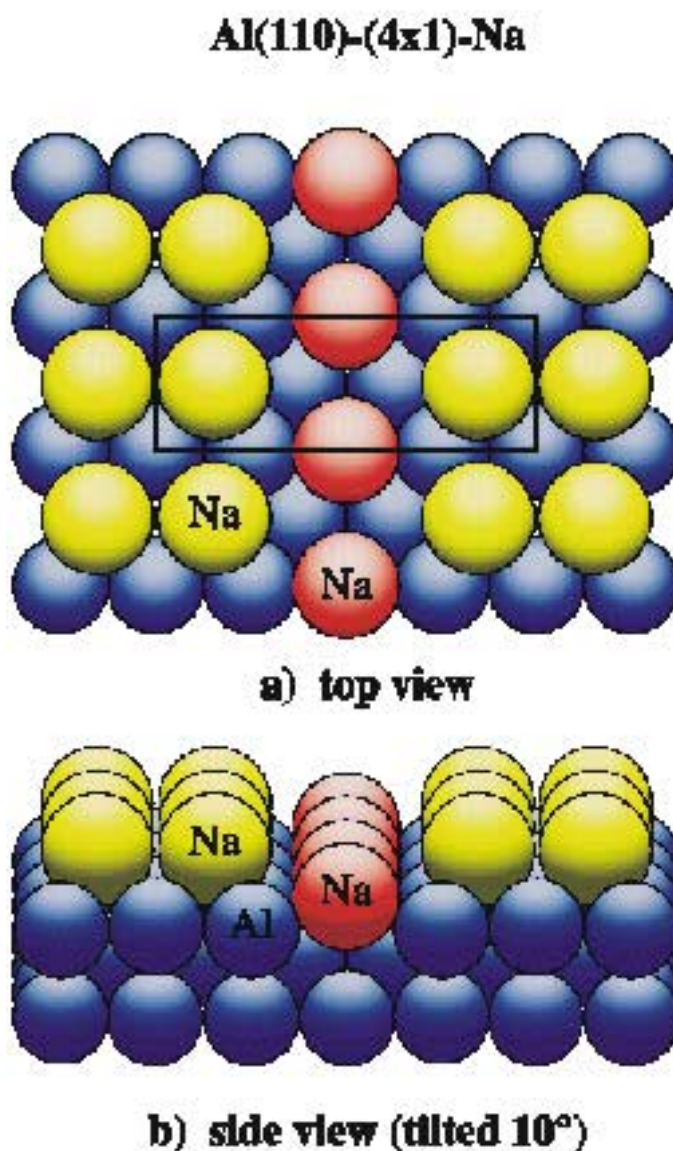


Fig. 4: Hard-sphere model of Al(110)- $(4\times 1)$ -Na structure. Al atoms are shown in blue. Substitutionally adsorbed Na atoms are shown in red. Chemisorbed Na atoms are shown in yellow. (a) Top view. The  $(4\times 1)$  unit cell is indicated in the panel. (b) Side view tilted by  $10^\circ$  from the plane of the paper.

#### 4.4.5 Structure of Al(110)–c(2×2)–Li and Formation of Surface Alloys

Lithium was deposited onto the aluminium crystal at room temperature from a thoroughly degassed source [4]. The deposition took about 2 minutes. The experimental conditions hold as in previous measurements. In order to minimize possible diffusion of Li into the bulk of the crystal, a clean Al(110) surface was, during days of repeated experiments, always prepared by first removing Li by sputtering before any heating of the crystal was carried out. Sharp c(2×2) LEED patterns with good contrast were obtained after deposition of 0.5 monolayer of Li at room temperature. The optimal coverage was found by measuring the ratio of integrated intensity in intensity spectra for integral and fractional-order beams as a function of coverage. The coverage was incremented until this ratio was at its maximum.

Al(110)–c(2×2)–Li			
	$\theta = 0^\circ$	$\theta = 10^\circ$	Average
$d_{01}$ [Å]	0.54±0.20	0.37±0.07	0.38±0.07
$d_{12}$ [Å]	1.25±0.02	1.25±0.02	1.25±0.01
$d_{23}$ [Å]	1.39±0.02	1.40±0.02	1.39±0.02
$d_{34}$ [Å]	1.36±0.03	1.35±0.02	1.36±0.02
$d_{45}$ [Å]	1.40±0.03	1.40±0.02	1.40±0.02
$d_{56}$ [Å]	1.39±0.03	1.40±0.03	1.39±0.02
$d_{67}$ [Å]	1.42±0.04	1.41±0.04	1.42±0.03
$\Delta r_3$ [Å]	0.11±0.02	0.11±0.02	0.11±0.01
$\Delta r_5$ [Å]	0.05±0.03	0.05±0.03	0.05±0.02
$u_0$ [Å]	0.50±0.20	0.28±0.10	0.35±0.10
$u_1$ [Å]	0.18±0.03	0.17±0.02	0.17±0.02
$u_2$ [Å]	0.17±0.04	0.15±0.03	0.15±0.02
$u_3$ [Å]	0.13±0.02	0.13±0.02	0.13±0.02
$u_4$ [Å]	0.09±0.04	0.08±0.03	0.09±0.03
$u_5$ [Å]	0.11±0.04	0.07±0.06	0.10±0.03
$u_{bulk}$ [Å]	0.09±0.03	0.10±0.04	0.10±0.02
$R$	0.039	0.062	

Tab. 6: Final parameter values for the Al(110)–c(2×2)–Li structure. The interlayer spacings and vibrational amplitudes are denoted  $d_{ij}$  and  $u_i$ , respectively, where the subscripts indicate the layers in question (0 belongs to the overlayer and 1 to the first layer of the substrate). The third and the fifth Al layers are split into bilayers with vertical splittings denoted by  $\Delta r_3$  and  $\Delta r_5$ .

The intensity spectra used for the analysis were taken at 100 K at normal incidence as well as  $\theta = 10^\circ$  incidence in the energy range 40–440 eV with a step

size 1 eV. Total number of different measured symmetry-inequivalent beams was 24 and 35 for  $\theta = 0^\circ$  and  $\theta = 10^\circ$ , respectively.

In dynamical LEED calculations, up to 324 partial waves and 383 plane waves (reduced by symmetry to 104 and 200 symmetry-adapted plane waves at  $\theta = 0^\circ$  and  $\theta = 10^\circ$ , respectively) were used in the  $L$ -space and  $k$ -space treatments, respectively, of multiple scattering within and between the atomic layers parallel to the surface.

The final revealed structure was very similar to the Al(110)-c(2×2)-Na and the same two-fold substitutional hard-sphere model hold. Numerical values of the structural parameters are listed in Tab. 6. Thus a detailed analysis indicates that Al(110)-c(2×2)-Li structure contains adsorbed Li atoms in a mixed Al/Li first layer forming a surface alloy. We assume that the displaced Al atoms are re-adsorbed at surface steps.

## 5 SUMMARY

Low-Energy Electron Diffraction (LEED) is one of the leading methods of surface science to determine the structures of well-ordered surfaces of solids. The work presented in this thesis has led to the following main results:

- *Establishing LEED in the laboratories of the Institute of Physical Engineering.* It involved both the building of an experimental apparatus (design, technical drawings, assembling and testing) and implementing the LEED methodology. Various methods of subtraction of background from the images of diffraction patterns were tested on both artificial and real images. It resulted in recommendation of the linear method and rejection of the expansion-of-minimum method. Kinematic theory of electron diffraction was extensively explored as a simpler alternative to the rigorous dynamical theory. Comparison of kinematic results with dynamical ones revealed that in spite of some good agreements, certain limits of the kinematic approach cannot be overcome, mainly the failure to describe the intensity of the fractional-order diffraction spots.
- *Determination of surface structures.* This task was aimed at alkali metal adsorption on Al(110) substrate. The structure of a clean Al(110) surface had been already known and hence, our new study concentrated at surface dynamics at 100 K and 300 K. A detailed analysis confirmed the surprising prediction of the recent *ab initio* calculations that vibrations of atoms in the second layer are larger than those in the first atomic layer. The structures Al(110)-c(2×2)-Na, Al(110)-(4×1)-Na and Al(110)-c(2×2)-Li had not been known and they were determined for the first time. The c(2×2)-Na phase is formed by a 1/2 monolayer adsorption of Na in two-fold substitutional sites with the displacement of a 1/2 monolayer of Al atoms from the top layer of the substrate. The reconstructive adsorption leads to strong perturbations of the substrate structure extending to the fifth atomic layer. The (4×1)-Na structure contains a 1/4 monolayer of Na atoms adsorbed in substitutional sites formed by the displacement of a 1/4 monolayer of

Al atoms from the first layer of the substrate, together with a 1/2 monolayer of Na atoms adsorbed in four-fold hollow sites on the first Al layer. The  $c(2\times 2)$ -Li structure is the same as for  $c(2\times 2)$ -Na although structural parameters are quantitatively different, of course. These three adsorption systems of Na and Li are the only well-ordered superstructures on an Al substrate in the given crystallographic orientation (there is no  $(4\times 1)$  phase for Li).

The doctoral thesis is based on papers listed below. A deep knowledge of adsorption geometries are of fundamental importance for the understanding of the adsorption systems. This is one of the actual objectives of surface science since the detailed nature of adsorption mechanisms is not known with certainty yet and the description of the nature of bonding in such structures is still open to discussion. The interplay between experiment and *ab initio* theories of adsorption is crucial for further development of this branch of science. Determining some of the surface structures is our modest contribution to the fascinating world of surface science.



## 6 ZÁVĚR

Difrakce pomalých elektronů (LEED) je jednou z hlavních metod vědy o površích a tenkých vrstvách pro určení povrchové struktury látek. Předložená práce přinesla následující hlavní výsledky:

- *Zavedení metody LEED do laboratoří Ústavu fyzikálního inženýrství VUT Brno.* To zahrnovalo jednak postavení aparatury včetně návrhu, tvorby technické dokumentace, montáže a oživení, jednak osvojení si metod elektronové difrakce. V rámci toho byly testovány různé metody odečtení pozadí z difrakčních obrazců. Porovnání bylo provedeno na základě řady umělých i skutečných difrakčních obrazců. Výsledkem bylo doporučení lineární metody odečtení pozadí a zamítnutí tzv. metody expanze minima. Rozsáhle byla zkoumána kinematická teorie elektronové difrakce jakožto jednodušší alternativa k rigorózní dynamické teorii. Porovnání kinematických a dynamických výsledků ukázalo, že navzdory určitým dobrým souhlasům nemohou být jistá omezení kinematické teorie překonána, zejména selhání popisu intenzity difrakčních stop neceločíselného řádu.
- *Určení povrchové struktury látek.* Tato část byla zaměřena na adsorpci alkalických kovů na povrchu vzorku Al(110). Struktura čistého krystalu Al(110) již byla předtím známa a naše nová studie se zaměřila na povrchovou dynamiku při 100 K a 300 K. Detailní analýza potvrdila překvapivou předpověď *ab initio* výpočtů, že vibrace atomů v druhé vrstvě jsou větší než v první atomové vrstvě. Struktury Al(110)-c(2×2)-Na, Al(110)-(4×1)-Na a Al(110)-c(2×2)-Li nebyly předtím známy a byly autorem určeny poprvé. Fáze c(2×2)-Na je tvořena adsorpcí 1/2 monovrstvy Na, která nahrazuje polovinu Al atomů první vrstvy substrátu. Substituční sodíkové atomy jsou „opřeny“ vždy o dva hliníkové atomy. Rekonstrukce povrchu vede k silným poruchám struktury substrátu zasahujícím až do páté atomové vrstvy. Superstruktura (4×1)-Na obsahuje 1/4 monovrstvy Na atomů adsorbovaných substitučně namísto 1/4 monovrstvy Al atomů první vrstvy substrátu, spolu s adsorpcí 1/2 monovrstvy Na atomů na této první Al vrstvě, kdy každý sodíkový atom je „opřen“ o čtyři hliníkové. Superstruktura c(2×2)-Li je totožná s c(2×2)-Na, ačkoliv kvantitativní hodnoty strukturních parametrů jsou samozřejmě odlišné. Tyto tři adsorpční systémy sodíku a lithia jsou jedinými dobře periodicky vyvinutými strukturami na povrchu hliníkového substrátu v dané krystalografické orientaci (pro lithium není žádná (4×1) fáze).

Disertační práce je založena na člancích citovaných níže. Znalost adsorpční geometrie je důležitá pro pochopení adsorpčních procesů. Je to jedno z aktuálních témat vědy o površích a tenkých vrstvách neboť podrobné mechanismy adsorpce dosud nejsou s jistotou známy a popis chemických vazeb v těchto strukturách je stále předmětem diskuse. Souhra experimentálních měření a *ab initio* teorií adsorpce je klíčová pro další vývoj této větve vědy o površích. Určení výše uvedených povrchových struktur je naším skromným příspěvkem k fascinujícímu světu vědy o površích.

## 7 AUTHOR'S PUBLICATIONS

### Papers published in international journals:

- [I] Jiruše, J., Šíkola, T. Application of simple kinematic predictions for the structural search in LEED. *Vacuum*. 1999, vol. 55, p. 141.
- [II] Mikkelsen, A., Jiruše, J., Adams, D. L. Structure and dynamics of the Al(110) surface. *Phys. Rev. B*. 1999, vol. 60, p. 7796.
- [III] Mikkelsen, A., Hoffmann, S. V., Jiruše, J., Adams, D. L. Surface reconstruction and relaxation of Al(110)-c(2×2)-Na. *Phys. Rev. B*. 2000, vol. 61, p. 13988.
- [IV] Mikkelsen, A., Petersen, J. H., Hoffmann, S. V., Jiruše, J., Adams, D. L. Structure and formation of surface alloys by adsorption of Li on Al(110). *Surf. Sci.* 2001, vol. 487, p. 28.
- [V] Mikkelsen, A., Petersen, J. H., Jiruše, J., Hoffmann, S. V., Adams, D. L. The surface structures formed by Na adsorption on A(110). *Surf. Sci.* 2002, vol. 497, p. 214.
- [VI] Roučka, R., Jiruše, J., Šíkola, T. Spot intensity processing in LEED images. *Vacuum*. 2002, vol. 65, no. 2, p. 121-126.

### Conference publications:

- [VII] Jiruše, J., Šíkola, T., Dub, P., Adams, D. L. Application of simple kinematic prediction for the structural search in LEED. In Olefjord, I. *Proc. of the 7th European Conference on Applications of Surface and Interface Analysis (ECASIA'97)*. Göteborg: Wiley & Sons, 1997, p. 868-871.
- [VIII] Roučka, R., Jiruše, J., Šíkola, T. Spot Intensity Processing in LEED Images. In Sanz, J. M., Espinoz J. P. *Abstracts of the 8th European Conference on Applications of Surface and Interface Analysis (ECASIA'99)*. Sevilla: poster presentation 4.-8. 10. 1999.

### Local publications:

- [IX] Šíkola, T., Dub, P., Jiruše, J., Nebojsa, A., Hájek, J., Češka, R. Particle scattering on solid surfaces. In *Proc. of the Workshop '96*. Brno: VUT Brno, 1996, p. 587.
- [X] Lopour, F., Kalousek, R., Jiruše, J., Roučka, R., Třískala, M., Tichopádek, P. In-situ Analysis of Surfaces and Thin Films II. In *MSMF-2*. Brno: VUT Brno, 1998, p. 64.
- [XI] Jiruše, J. Analýza struktury povrchů materiálů metodou difrakce pomalých elektronů (LEED). In *II. sborník příspěvků doktorandů, konference u příležitosti 100. výročí založení FSI*. Brno: VUT Brno, 2000, p.121 – 124 (in Czech).

## 8 REFERENCES

- [1] Pendry, J. B. *Low Energy Electron Diffraction*. London: Academic, 1974.
- [2] Van Hove, M. A., Weinberg, W. H., Chan, C. M. *Low-Energy Electron Diffraction*. Berlin: Springer-Verlag, 1986.
- [3] Davisson, C. J., Germer, L. H. *Phys. Rev.* 1927, vol. 30, p. 705.
- [4] SAES Getters, <http://www.saesgetters.com>.
- [5] Moruzzi, V. L., Janak, J. F., Williams, A. R. *Calculated Electronic Properties of Metals*. New York: Pergamon, 1978.
- [6] Titterington, D. J., Kinniburgh, C. G. *Comp. Phys. Com.* 1980, vol. 20, p. 237.
- [7] Van Hove, M. A., Tong, S. Y. *Surface Crystallography by LEED*. Berlin: Springer, 1979.
- [8] Adams, D. L. *J. Phys. C* 1983, vol. 16, p. 6101.
- [9] Adams, D. L., Jensen, V., Sun, X. F., Vollesen, J. H. *Phys. Rev.* 1988, vol. B 38, p. 7913.
- [10] Guo, T., Atkinson, R. E., Ford, W. K. *Rev. Sci. Instrum.* 1990, vol. 61, p. 968.
- [11] Toofan, J., Watson, P. R. *Rev. Sci. Instrum.* 1994, vol. 65, p. 3382.
- [12] Lang, E., Heilmann, P., Heinz, K., Müller K. *Appl. Phys.* 1976, vol. 9, p. 247.
- [13] Russ, J. C. *The Image Processing Handbook*. Boca Raton: CRC Press, 1995.
- [14] Nielsen, M. M., Burchhardt, J., Adams, D. L. *Phys. Rev.* 1994, vol. B 50, p. 7851.
- [15] Nielsen, M. M., Burchhardt, J., Adams, D. L., Lundgren, E., Andersen, J. N. *Phys. Rev.* 1994, vol. B 50, p. 4718.
- [16] Marquardt, D. W. *J. Soc. Ind. Appl. Mat.* 1963, vol. 11, p. 431.
- [17] Fritzsche, V., Pendry, J. B., Löffler, U., Wedler, H., Mendez, M. A., Heinz, K. *Surf. Sci.* 1993, vol. 289, p. 389.
- [18] Jepsen, D. W., Marcus, P. M., Jona, F. *Phys. Rev.* 1972, vol. B 5, p. 3933.
- [19] Marzari, N., Vanderbilt, D., Vita, A. D., Payne, M. C. *Phys. Rev. Lett.* 1999, vol. 82, p. 3296.
- [20] Taylor, A., Kagle, B. J. *Crystallographic Data on Metal and Alloy Structures*. New York: Dover, 1963.
- [21] Bonzel, H. P., Bradshaw, A. M., Ertl, G. *Physics and Chemistry of Alkali Metal Adsorption*. Amsterdam: Elsevier, 1989.

## 9 CURRICULUM VITAE

Name: Jaroslav Jiruše

Date and place of birth: 22<sup>nd</sup> May 1973 in Brno

Address: Dvorská 22, Blansko 678 01

Education:

1987-1991 Grammar school in Blansko

1991-1996 Brno University of Technology, Faculty of Physical Engineering  
since 1996 PhD course

I graduated at Brno University of Technology with honours and obtained the Dean's award and academic degree Ing. (M. Sc.). Already during my study I established cooperation with Aarhus University in Denmark where I spent 6 month dealing with Low-Energy Electron Diffraction. After the graduation I started PhD course continuing naturally the same subject matter. From the beginning I participated in various grant projects and I was also a member of the academic senate. After two and half year I passed the state rigorous exam and defended the PhD thesis outline. Then I interrupt the PhD course and fulfilled the military duties. After that, in 2000, I entered a job in Grafitec firm (a producer of the offset printing machines) where I worked on project of imaging the printing plate by laser diodes. In the meantime I published results of my PhD research and prepared the final thesis.

I am fluent in both written and spoken English and Russian, and I have a basic knowledge of German. I am skilled in working with PC.